Caldesmon effects on the actin cytoskeleton and cell adhesion in cultured HTM cells

Inna Grosheva [a,1], Jason L. Vittitow [b], Polina Goichberg [a], B'Ann True Gabelt [c,*],
Paul L. Kaufman [c], Terete Borrás [b], Benjamin Geiger [a], Alexander D. Bershadsky [a]

[a] *Department of Molecular Cell Biology, Weizmann Institute of Science, Rehovot 76100, Israel*
[b] *Department of Ophthalmology, University of North Carolina, 6109 NeuroSci Res Building, Box 7041, Chapel Hill, NC, USA*
[c] *Department of Ophthalmology & Visual Sciences, University of Wisconsin, 600 Highland Avenue, F4/340 CSC, Madison, WI 53792, USA*

Abstract

Caldesmon is a multifunctional ubiquitous regulator of the actin cytoskeleton, which can affect both actomyosin contractility and actin polymerization. Previous studies showed that caldesmon over-expression in cultured fibroblasts produces effects that resemble those of chemical inhibitors of cellular contractility. Since these inhibitors (H-7, Y-27632, etc.) have been shown to lower intraocular pressure and increase outflow facility from the anterior chamber of the eye, we proposed that caldesmon might be used for gene therapy of glaucoma. In the present study we examined the effects of expression of adenovirus-delivered rat non-muscle caldesmon fused with green fluorescent protein (AdCaldGFP) on the actin cytoskeleton and matrix adhesions in cultured human trabecular meshwork (HTM) cells. In addition, we assessed the effect of caldesmon on the stability of cell–cell junctions in kidney epithelial MDCK cells. Cultured HTM cells demonstrate a well-developed actin cytoskeleton, comprising mainly arrays of parallel actomyosin bundles (stress fibers). Lamellipodial protrusions containing dense actin networks are also observed. Cell–matrix adhesions are dominated by focal adhesions (FAs) associated with the ends of the stress fibers, focal complexes in lamellipodia, and fibrillar adhesions in the central part of the spread cells. Treatment of HTM cells with AdCaldGFP resulted in dose-dependent morphological changes within 24–48 hr post-infection. Cells expressing moderate levels of caldesmon exhibited straight bundles containing actin and myosin II, which were considerably shorter than those in control cells. Short filament bundles in caldesmon over-expressing cells formed arrays consisting of triangular actin structures with small vinculin-positive FAs at their vertices. In addition, the fraction of cells displaying large lamellipodia increased. About 40–50% of the population of caldesmon-expressing cells demonstrated high levels of GFP–caldesmon expression and severe changes in the actin cytoskeleton, manifested by the disappearance of stress fibers and the formation of curved actin- and myosin-containing bundles. These bundles formed together a dynamic network consisting of pulsating loops filling the entire cytoplasm. Addition of thapsigargin, which increases intracellular Ca^{++} concentration, resulted in a straightening of the curved bundles. Another type of novel actin structures induced by caldesmon over-expression were highly dynamic circular waves that propagated over the affected cells with a velocity about 10 µm min. In cells with disrupted stress fibers, vinculin-containing FAs and tensin-rich fibrillar adhesions had also essentially vanished. However, phosphotyrosine-positive focal complexes were still prominent throughout the lamellipodia of these cells. Over-expression of caldesmon in MDCK cells reduced, in a dose dependent manner, the beta-catenin content at cell–cell adherens junctions and in some cases led to physical disruption of adherens junctions. Thus, caldesmon over-expression induces unique reorganization of the actin cytoskeleton in affected cells, accompanied by disruption of focal and fibrillar cell–matrix adhesions, and destabilization of cell–cell adherens junctions. Inducing such changes in the contractility and actin cytoskeleton of HTM cells in glaucomatous eyes in vivo could produce a therapeutically useful increase in outflow facility.
© 2006 Elsevier Ltd. All rights reserved.

---

* Corresponding author. B.T. Gabelt, Department of Ophthalmology & Visual Sciences, University of Wisconsin, 600 Highland Avenue, F4/340 CSC, Madison, WI 53792, USA.

E-mail addresses: ing2001@med.cornell.edu (I. Grosheva), jvittitow@inspirepharm.com (J.L. Vittitow), polina.goichberg@weizmann.ac.il (P. Goichberg), btgabelt@wisc.edu (B.'A.T. Gabelt), kaufmanp@mhub.ophth.wisc.edu (P.L. Kaufman), tborras@med.unc.edu (T. Borrás), benny.geiger@weizmann.ac.il (B. Geiger), alexander.bershadsky@weizmann.ac.il (A.D. Bershadsky).

[1] Present address: Department of Biochemistry, Weill Medical College of Cornell University, 1300 York Avenue, New York, NY 10021, USA.

1. Introduction

Caldesmon is a ubiquitous component of the actin cytoskeleton that may regulate several aspects of its organization and function. In smooth muscle, caldesmon is one of the most abundant proteins and an important effector of Ca^{++}-mediated contractility regulation. Caldesmon forms a complex with actin, myosin II, and tropomyosin and inhibits actin-activated myosin ATPase activity (reviewed in (Huber, 1997; Chalovich et al., 1998; Marston et al., 1998)). Ca^{++}-calmodulin binding to caldesmon abolishes this inhibition, triggering the motor activity of myosin II. Thus, in smooth muscle, caldesmon plays a regulatory role, similar to that of troponin in striated muscle. Smooth muscle and non-muscle caldesmon are expressed from a single gene via alternative RNA splicing (Hayashi et al., 1992; Payne et al., 1995) and except for the lack of a central 'spacer' domain, non-muscle caldesmon contains all the functionally important domains of the muscle-derived molecule. Therefore, it is tempting to speculate that in non-muscle cells, caldesmon also regulates cell contractility, albeit unequivocal evidence of that is still missing (Dabrowska et al., 2004). It was, however, shown that over-expression of exogenous caldesmon in cultured cells reduces their contractility, which leads to profound reorganization of the actin cytoskeleton and cell–matrix adhesions (Helfman et al., 1999).

Myosin II-driven contractility plays a crucial role in the assembly and maintenance of two domains of the actin cytoskeleton, stress fibers and associated focal adhesions (FAs) that link the actin cytoskeleton to the extracellular matrix. They are comprised of integrin-type transmembrane receptors and of a number of structural and signaling proteins associated with the cytoplasmic domains of integrins (reviewed in (Geiger et al., 2001)). Formation of stress fibers and FAs in the cell is triggered by small GTPase Rho, which activates members of the Rho-associated kinase family (Burridge and Wennerberg, 2004). These enzymes (in particular, ROCK I (Yoneda et al., 2005)) positively regulate myosin light chain (MLC) phosphorylation by phosphorylating and inactivating myosin light chain phosphatase (MLCP) and, in some cases, by directly phosphorylating MLC (Fukata et al., 2001). MLC phosphorylation is critical for stress fiber and FA formation, and a variety of chemical inhibitors of ROCK and of myosin light chain kinase (MLCK) were shown to disrupt these structures (Volberg et al., 1994; Chrzanowska-Wodnicka and Burridge, 1996; Riveline et al., 2001). Myosin II activity is required for the formation and maintenance of focal adhesions because these structures are mechanosensitive and can assemble only upon application of mechanical force (Riveline et al., 2001; Bershadsky et al., 2003). Caldesmon works downstream from MLC phosphorylation and inhibits myosin II on the level of its interaction with actin (Okagaki et al., 1991; Shirinsky et al., 1992). As a result, in the presence of excess caldesmon, myosin II activity is suppressed, mechanical force is not applied to the focal adhesions and they disassemble (Helfman et al., 1999).

Similarity between cellular effects of chemical inhibitors of myosin II and caldesmon is important in the context of possible glaucoma therapy development. These inhibitors (e.g. H-7, ML-7, Y-27632 and others) as well as the actin depolymerizing drugs, latrunculins A and B, have been shown to either lower intraocular pressure and/or increase outflow facility in vitro and/or in vivo (Epstein et al., 1999; Peterson et al., 1999, 2000; Tian et al., 2000, 2004; Honjo et al., 2001; Rao et al., 2001, 2005; Tian and Kaufman, 2005) and therefore are potentially applicable for the pharmacotherapy of glaucoma. However, the possibility of bypassing the external agent and 'setting' the outflow tissue to a higher facility level using genetic tools would have the great advantage of eliminating the need for repetitive drug application. As shown in an accompanying paper (Gabelt et al., this volume), caldesmon over-expression, indeed, increases outflow facility in organ-cultured human and monkey anterior segments.

However, caldesmon effects on the cytoskeleton are different in many ways from those produced by MLC phosphorylation inhibitors and actin depolymerizing drugs. Recent in vitro studies revealed that, in addition to its effect on myosin ATPase, caldesmon can affect organization of the actin cytoskeleton via different mechanisms. First, caldesmon, together with its partner, tropomyosin, efficiently competes with the actin filament cross-linking protein, fascin, and, therefore, may prevent formation of some classes of actin bundles (Ishikawa et al., 1998). Moreover, caldesmon inhibits the binding of the Arp2/3 actin-nucleating complex to actin filaments, preventing the formation of a branching actin network and inhibiting Arp2/3-mediated actin nucleation (Yamakita et al., 2003).

Caldesmon activity is precisely regulated in the cell. In particular, caldesmon is negatively regulated by Ca^{++}-calmodulin; a caldesmon mutant defective in Ca^{++}-calmodulin binding interferes severely with the assembly of stress fibers and focal adhesions in CHO cells (Li et al., 2004). In addition, caldesmon can be phosphorylated at several serine–threonine and perhaps tyrosine residues and is a target for several important protein kinases (review (Dabrowska et al., 1996)). In particular, a key cyclin-dependent kinase, Cdc2, regulates caldesmon phosphorylation in the cell cycle (Yamashiro et al., 2001; Li et al., 2003) and upon integrin signaling (Manes et al., 2003). A caldesmon mutant lacking Cdc2 phosphorylation sites demonstrates a significantly more severe phenotype than the wild-type protein upon transfection into fibroblasts (Yamashiro et al., 2001).

This versatility in possible functions and in the pathways of regulation suggests that in different cell types and physiological conditions, caldesmon over-expression can produce different effects. Therefore, the possible use of caldesmon in glaucoma gene therapy requires detailed investigation of its effects on cell parameters potentially related to the control of aqueous humor outflow, namely organization of the actin cytoskeleton, cell matrix adhesions and cell–cell adherens junctions. In this study, we determined the effects of GFP–caldesmon delivery on the actin cytoskeleton and matrix adhesions in cultured human trabecular meshwork (HTM)

cells, and on cell–cell adherens junctions in MDCK epithelial cells, a classic test model for cell–cell junction studies.

2. Materials and methods

2.1. HTM cells

Primary HTM cells were isolated from non-glaucomatous human donor eyes within 48 hr of death. All procedures were in accordance with the Tenets of the Declaration of Helsinki. For isolation of HTM cells, the TM from a single individual was isolated from surrounding tissue by making incisions both anterior and posterior to the meshwork and removing it using forceps. The tissue was then cut into small pieces, treated with 1 mg/ml collagenase in phosphate buffered saline (PBS) and incubated at 37°C in a shaker water-bath for 1 hr. Incubation was followed by low speed centrifugation for 5 min. Pellets were re-suspended in 4 ml of Improved Minimal Essential Medium (IMEM; Biofluids, Rockville, MD) supplemented with 20% fetal bovine serum (FBS) and 50 μg/ml gentamicin (GIBCO Invitrogen, Carlsbad, CA). Resuspended tissue was plated on a single, 2% gelatin-coated 35 mm dish and maintained in a 37°C, 7% CO_2 incubator. Once confluent (2–3 weeks), cells were passed to a T-25 flask and labelled as passage 1. Subsequently, cells were passed 1:4 at confluency and maintained in the same medium with 10% FBS (complete IMEM). Cells used for experiments were at passages 3–5.

These outflow pathway cultures comprise all cell types involved in maintaining resistance to flow. These include cells from three distinct regions of the TM plus cells lining Schlemm's canal. Because most of the cells in these cultures come from the TM, they are commonly referred to as 'primary non-transformed' TM cells. In some experiments, cells of the immortalized TM-1 line (Filla et al., 2002) obtained from HTM by transfection with an SV40 origin defective vector (Murnane et al., 1985) were used. All cultures were grown in DMEM medium supplemented with 10% FBS. Cells were dissociated by trypsinization and replated either on Petri dishes with coverslips placed onto the bottom (for subsequent fixation and immunofluorescence staining), or on glass-bottomed dishes for live cell observations and filming. For the majority of the experiments, confluent cultures of HTM cells were split 1:4 for replating. Twenty-four hours after replating the cells were infected with the adenoviruses encoding GFP–caldesmon or GFP (see below, Section 2.2) and examined 24 hr after infection. At that time, about 90% of cells were positive for GFP-fluorescence.

2.2. RNA extraction

For the cells, RNA extraction was performed by resuspending cellular pellets in guanidine thiocyanate buffer (RLT, QIAGEN, Valencia, CA) and loading the solution onto a QIAshredder column followed by the use of the RNeasy Mini kit with on-column RNase-free DNase digestion (QIAGEN). Total RNA recoveries averaged 30 μg per 10 cm plate, respectively. For the tissues, excised human TMs from perfused anterior segments were homogenized individually with 350 μl RLT (QIAGEN) in a glass micro tissue grinder (Kimble-Kontes, Vineland, NJ) prior to loading onto the QIAshredder column. Total RNA averaged 2 μg per individual TM, which was eluted in 30 μl RNase-free water.

2.3. Determination of caldesmon expression in HTM cells and human TM tissue

Total RNA from HTM cells or TM tissue was hybridized to Human Genome U95Av2 ($n=7$) or U133A GeneChip microarrays ($n=2$) (Affymetrix, Santa Clara, CA) at either Duke University (2) or the University of North Carolina Chapel Hill (UNC) Core Facilities (7). For the cells, 7 μg of total RNA were reverse transcribed to cDNA using a custom cDNA kit (Life Technologies) with a T7-$(dT)_{24}$ primer. Biotinylated cRNA was then generated from the cDNA reaction using the BioArray High Yield RNA Transcript Kit. For the small quantities of the TM tissue, 100 ng of total RNA was used to generate cDNA in the first cycle cDNA synthesis with T7-Oligo (dT) promoter primer and Invitrogen cDNA reagents. First cycle in vitro transcription for cRNA amplification was carried out using the Ambion MEGAscript T7 Kit. Second cycle cDNA synthesis was carried out using Invitrogen cDNA reagents. Second cycle IVT for cRNA amplification was carried out using the ENZO BioArray HighYield RNA Transcript Labeling Kit.

The cRNAs were then fragmented in fragmentation buffer at 94°C for 35 min and added to a hybridization cocktail containing 0.05 μg/μl fragmented cRNA, 50 pM control oligonucleotide B2, BioB, BioC, BioD, Cre hybridization controls and 0.1 mg/ml herring sperm DNA. Arrays were hybridized (16 hr at 45°C in the GeneChip Hybridization Oven 640), washed and stained with R-phycoerythrin streptavidin in the GeneChip Fluidics Station 400. After this, the arrays were scanned with the Hewlett Packard GeneArray Scanner. Sample quality was assessed by examination of $3'$ to $5'$ intensity ratios of certain genes, and Affymetrix GeneChip Microarray Suite 5.0 software was used for scanning and basic analysis.

2.4. Adenoviral vector construction

AdCaldGFP, a replication-deficient recombinant Adenovirus (Ad) encoding the rat caldesmon protein was generated as described in the accompanying paper (Gabelt et al., this volume). The expression cassette cDNA of this virus contains a fusion of the green fluorescent protein (GFP) cDNA (nucleotides (nt) 284–1001 GenBank accession number U76561) with the coding region of the rat caldesmon cDNA (nt 724–2319 GenBank accession number NM013146).

2.5. MDCK cells and their transfection

Cells of the Madin Darby canine kidney (MDCK) cell line were maintained in DMEM supplemented with 10% heat inactivated FBS, glutamine and antibiotics, at 37°C in a humidified atmosphere containing 7% CO_2. Cells were plated

for 18 hr on glass coverslips at a density of 1×10^5 cells per 35 mm dish, transfected with 2 μg DNA using 4 μl Lipofectamine reagent (GibcoBRL, Life Technologies, UK) according to the manufacturer's instructions, fixed and immunolabeled 24 hr after transfection, as described below. The preparation of vectors expressing GFP-tagged wild type or truncated non-muscle caldesmon was previously described (Helfman et al., 1999).

2.6. Fluorescence microscopy

Cells were fixed and subjected to immunofluorescence staining of cytoskeletal proteins. Usually, after brief rinsing in PBS at 37°C, cells were fixed with 3% paraformaldehyde in PBS for 20–30 min at room temperature. After fixation, cells were rinsed with PBS and permeabilized with 0.5% of Triton X-100 in PBS for 5 min. When a higher degree of permeabilization was required (e.g. for myosin II visualization in HTM, or for β-catenin–caldesmon staining in MDCK cells), the cells were first fixed with a mixture containing 0.5% Triton X-100 and 3% paraformaldehyde in PBS for 2–3 min and then post-fixed with 3% paraformaldehyde for 20 min. To visualize F-actin, cells were subsequently incubated with 100 nM TRITC-phalloidin (Sigma, St Louis, MO, USA); for antibody-staining, cells were incubated with primary antibodies diluted in PBS. Cells were then washed in PBS three times and incubated with the secondary, fluorochrome-conjugated antibodies. Nuclei were stained with 2.5 μg/ml DAPI (4′,6-diamidino-2-phenylindole, Sigma) added to the secondary antibody solution. After three final washes, the coverslips were mounted in Elvanol (Mowiol 4-88, Hoechst, Germany). The following primary antibodies were used in this study. Rabbit anti-β-catenin, monoclonal anti-vinculin (hVin), and monoclonal anti-MLC (Myosin Light Chain), clone M22, were from Sigma Immunochemicals, Ltd. (Rehovot, Israel). Vinculin antibody was used at a dilution of 1:200 and anti-MLC antibody at a dilution of 1:50. Monoclonal anti-tensin was purchased from Transduction Laboratories (Lexington, KY, USA) and used at a 1:25 dilution (10 μg/ml). Polyclonal anti-phosphotyrosine antibody (PT40) was kindly provided by Prof. Israel Pecht (Department of Immunology, Weizmann Institute of Science, Rehovot, Israel). Secondary goat anti-mouse and anti-rabbit antibodies coupled to Cy-3, or Cy-5 were purchased from Jackson Laboratories (West Grove, PA), Alexa-350 and Alexa-488 conjugated antibodies were from Molecular Probes Inc. (Eugene, OR).

2.7. Image acquisition and analysis

Images were recorded on an Axiovert 100 TV inverted microscope (Zeiss, Oberkochen, Germany) equipped with a 100 W mercury lamp, a $100 \times /1.4$ plan-Neofluar objective (Zeiss, Oberkochen, Germany), excitation and emission filter wheels, and a CCD Camera (CH300/CE 350, Photometrics, Tucson, AZ) with KAF1400 CCD chip, controlled by a DeltaVision system (Applied Precision, Inc., Issaquah, WA).

To quantify fluorescence intensities at the cell–cell adherens junctions, immunofluorescence images were acquired by the DeltaVision system using Resolve3D software (Applied Precision, Inc., Issaqua, WA, USA). The digital images obtained were high pass filtered using Priism software as described (Zamir et al., 1999), and segmented by thresholding to produce a binary cut-off mask that included the cell–cell contacts. This mask was applied to the original image to calculate integrated intensity in the segmented region and the background below the threshold value. Integrated intensity of AJ labeling per field was normalized by dividing by the number of cells in the field (counted using DAPI nuclear labeling).

2.8. Live cell recording

GFP-caldesmon-expressing cells growing in glass-bottomed dishes (MatTek Corporation, Ashland, MA, USA) in HEPES (25 mM) buffered growth medium were examined using the Axiovert 100 TV microscope described above equipped with Box and Temperature control system from Life Imaging Services (Switzerland, www.lis.ch/). Filters for detection of GFP were from Chroma (Chroma Technology Corp, Rockingham, VT). Time-lapse recordings of cells were performed at 1-min intervals. In experiments with thapsigargin (Sigma), the drug was added to the medium to a final concentration 2 μM.

3. Results

3.1. Endogenous expression of caldesmon in HTM cells

Endogenous caldesmon expression was analysed on Affymetrix chips in primary human TM cells ($n = 4$) and intact human TM from perfused anterior segments from post-mortem donors ($n = 4$). Four human cell lines were used at passage 5 and were each derived from different male and female Caucasian and African–American individuals, ranging in age from 19 to 39 years old. The perfused tissue was obtained from male and female Caucasian, Hispanic and African- donors ranging in age from 78 to 87 years old. The U95v2 chips ($n = 6$) contain each two hybridization spots corresponding to human caldesmon cDNA (GenBank access nos. M64110 and M83216). The U133A chips ($n = 2$) each contain five hybridization spots corresponding to human caldesmon cDNA (GenBank access nos. M64110.1, AI685060, AL577531, AL583520 and D90453). Use of Affymetrix algorithms on the signals given after hybridization to the caldesmon spots (see Section 2) resulted in a total of 20 'Present' out of the total 22 analyzed (Table 1). The p values of the 'present' spots were highly significant ($p \leq 0.001$) while those of the two 'absent' spots were not ($p \geq 0.09$). The expression of caldesmon did not depend of age, race or gender (Table 1). Although expression levels of caldesmon in comparison to the expression of another gene were not measured, the strength of the signal obtain suggests that caldesmon expression appears among the 25% of the genes on the chip with the highest signal strengths.

Table 1
Endogenous caldesmon (CALD1) expression in human TM

GenBank acc. no.[a]	Gene chip	Signal	P-Value	Absent/present
Primary human TM cells				
M64110	U95v2-1	3313	0.00022	P
	U95v2-2	3428	0.00022	P
M64110.1	U133A-1	2026	0.00024	P
	U133A-2	2544	0.00024	P
M83216	U95v2-1	2905	0.00022	P
	U95v2-2	3662	0.00022	P
AI685060	U133A-1	3434	0.00024	P
	U133A-2	1479	0.00195	P
AL577531	U133A-1	2066	0.00024	P
	U133A-2	4339	0.00024	P
AL583520	U133A-1	8035	0.00024	P
	U133A-2	9721	0.00024	P
D90453	U133A-1	235	0.03027	P
	U133A-2	234	0.09522	A
Perfused human TM tissue				
M64110	U95v2-3	1240	0.00022	P
	U95v2-4	2401	0.00022	P
	U95v2-5	578	0.01145	P
	U95v2-6	1720	0.00022	P
M83216	U95v2-3	195	0.00160	P
	U95v2-4	403	0.00022	P
	U95v2-5	147	0.26746	A
	U95v2-6	354	0.00039	P

RNA from four different primary TM cell lines and four perfused TM tissues hybridized to Affychips U95v2 and U133A.

[a] All GenBank accession numbers belong to Unigene Hs.490203.

3.2. Actin cytoskeleton and matrix adhesions in control HTM cells

All experiments with HTM cells described in this and in the following paragraphs were performed on two independent primary cultures. The results were identical for both batches of cells. Sparse or sub-confluent cultures of HTM cells were studied. Two major forms of actin-containing structures were revealed in these cells by staining with fluorescently labeled phalloidin: parallel actin cables in the cell body, and actin-rich rims at the edge of lamellipodial protrusions. Actin cables (stress fibers) were prevalent in these cells. They formed one or few densely packed parallel arrays traversing the entire cell (Fig. 1A and C). Besides actin, the stress fibers are known to contain a variety of actin-associated proteins. In particular, a characteristic feature of the stress fibers is the presence of molecular motor myosin II, as revealed by staining with the antibody to myosin II regulatory light chain (MLC) (Fig. 1B). Staining for myosin II revealed typical 'striations' in its distribution along the stress fibers. Moreover, similar to several other cell types (Svitkina et al., 1986; Verkhovsky et al., 1995), striated myosin II patterns in HTM cells were often seen not only in the distinctly prominent stress fibers, but also over the large cell areas (myosin sheaths), where myosin II was apparently associated with densely packed thin actin fibers (Fig. 1B).

Lamellipodia were not often seen in the HTM cells, presumably because these cells were barely motile in our culture conditions. In particular, at 48 h after plating, the cells still had free edges, but most did not form lamellipodia and ruffles at the periphery. Nevertheless, in the cases when the lamellipodia and ruffles were observed (Fig. 1A and C), they demonstrated characteristic bright actin staining corresponding to the dense branching actin network known to fill these structures (Small et al., 2002). Myosin II was not detectable at the peripheral lamellipodial protrusions of the HTM cells by staining with the MLC antibody (Fig. 1B)

Staining of the HTM cells for vinculin, -tensin, and -phosphotyrosine was used to characterize the organization of the cell–matrix adhesions. The major type of adhesion structures in the HTM cells are 'classic' FAs (Geiger et al., 2001)—elongated plaques with approximate width and length of 0.5–1.0 and 2–5 μm, respectively—readily visualized by vinculin antibody staining (Fig. 1D). FAs are associated with the ends of actin- and myosin II-containing stress fibers and usually accumulate at the cell periphery. FAs are known to evolve from small dot-like focal complexes that continuously appear underneath the lamellipodial protrusions (Geiger et al., 2001). In HTM cells, vinculin positive dot-like focal complexes were observed in association with peripheral lamellipodia (Fig. 1D). Both focal adhesions and focal complexes in HTM cells are enriched in tyrosine phosphorylated proteins which were visualized by the antibody to phosphotyrosine (not shown).

Tensin is a marker for the special type of matrix adhesion known as fibrillar adhesions, which, in fibroblasts, are localized at the central part of the cell, associate with fibronectin fibers and do not contain tyrosine phosphorylated proteins (Zamir et al., 1999). Combined staining with antibodies to tensin and phosphotyrosine revealed adhesions of this type also in HTM cells. These adhesions were tensin positive, but phosphotyrosine negative, and sometimes associated with the stress fibers along their length (Fig. 1E and F).

3.3. Novel types of actin structures induced by caldesmon over-expression

GFP-caldesmon expressed in HTM cells decorated all actin-containing structures, including stress fibers and other actin filament bundles, ruffles, lamellipodia, etc. (Figs. 2, 4 and 5). At the same time, the actin cytoskeleton in cells over-expressing caldesmon, underwent major reorganization. It was convenient to subdivide these changes in actin organization into two groups: moderate reorganization presumably induced by relatively low levels of caldesmon over-expression, and severe reorganization usually associated with high-level caldesmon over-expression.

Cells with mild reorganization of the actin cytoskeleton still contained straight bundles of actin filaments (Figs. 2 and 3) decorated by myosin II striations (Fig. 2C and D). In GFP-caldesmon-expressing cells, which preserve apparently intact stress-fibers, vinculin-containing FAs were also well preserved. Superimposition of GFP-caldesmon and vinculin images in the same cell revealed that GFP-caldesmon not only localized to the stress fibers, but intensely co-localized with vinculin in many FAs. In some cases GFP-caldesmon was
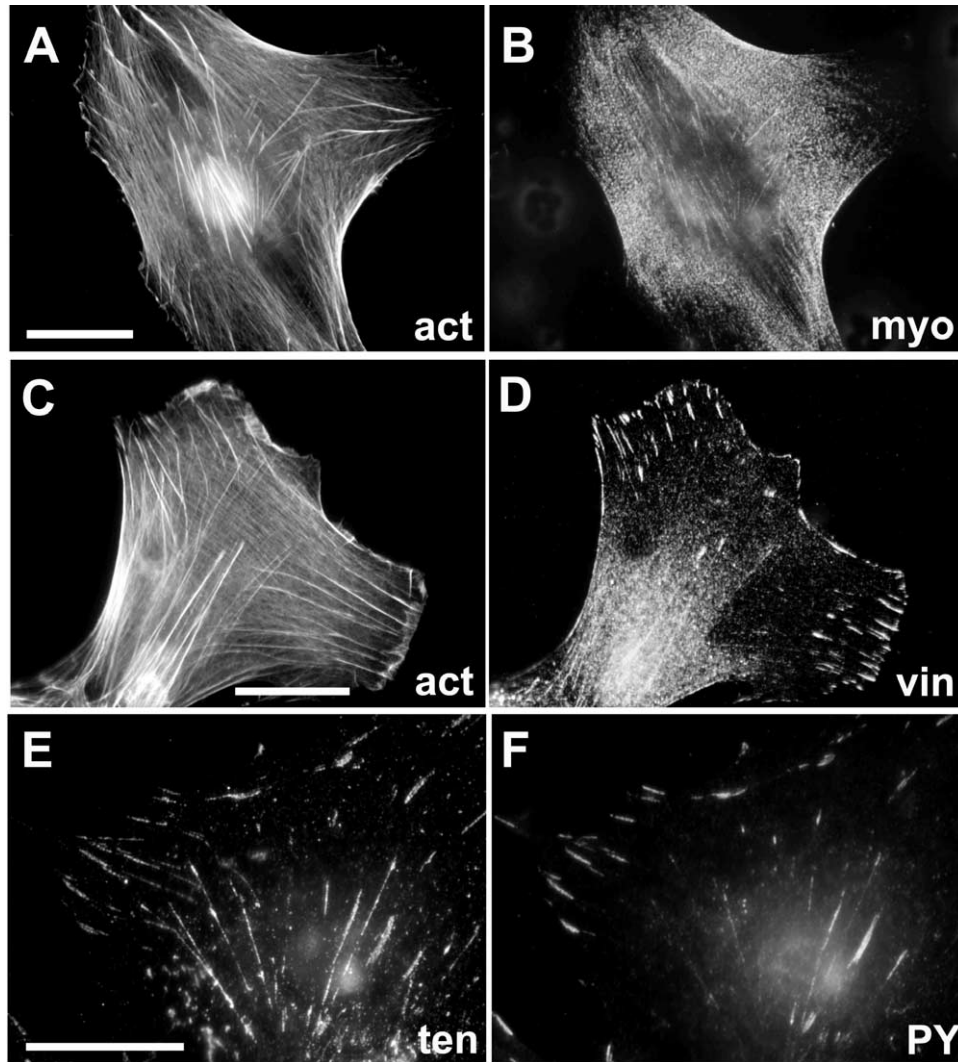
Fig. 1. Typical organization of the actin cytoskeleton and cell–matrix adhesions in control HTM cells. (A) Phalloidin staining reveals polymerized actin (act) in long, straight actin filament bundles (stress fibers); (B) staining with antibody to myosin light chain (myo) reveals myosin II striated distribution along the stress fibers in the same cell. (C) Phalloidin staining shows actin (act) in stress fibers and peripheral lamellipodia; (D) vinculin antibody staining (vin) visualizes numerous elongated focal adhesions associated with the ends of stress fibers and small dot-like focal complexes associated with lamellipodia at the cell edges. (E) Staining with tensin antibody (ten) shows focal adhesions at the cell periphery and fibrillar adhesions in the central part of the cell; (F) focal, but not fibrillar adhesions are enriched in tyrosine-phosphorylated proteins visualized by phosphotyrosine (PY) antibody staining. Scale bars: 20 μm.

distributed over the entire area of the FA, otherwise it occupied the proximal, stress-fiber-associated regions of the FA (Fig. 3A–C)

Instead of parallel arrays going through the entire cells, the short filament bundles in caldesmon-expressing cells formed triangular arrays (Fig. 3D). Vinculin was located at the vertices of these triangles together with caldesmon and sometimes faintly labeled the bundles themselves (Fig. 3E and F). Thus, such cells, unlike the control ones, displayed numerous vinculin-containing FAs at the center rather than at the cell periphery. In addition to the short stress-fiber like bundles, thinner curvy actin- and caldesmon-positive fibers were often seen in these cells (Fig. 2A and 3D). These fibers were loosely connected to the neighboring stress-fiber like bundles.

About 40–50% of the population of caldesmon over-expressing cells demonstrated severe changes in the actin cytoskeleton. These cells displayed entirely different types of actin structures as compared to control HTM cells (Fig. 4). Stress-fiber like bundles were completely absent. Numerous actin filament bundles in these cells were curvilinear and formed a network consisting of interconnected loops filling the whole cytoplasm (Fig. 4A and B). This network was dynamic as could clearly be seen in the time-lapse observation of GFP-caldesmon taken with 1-min intervals between the frames (Movie 1). Time-lapse movies show that curved fibers were motile and underwent continuous pulsation and remodeling i.e. fusion of fibers, formation of new loops, etc. This severe reorganization of the actin cytoskeleton did not inhibit cell motility. On the contrary, TM-1 cells infected with GFP-caldesmon, in which all actin bundles were curved, were very motile and directionally locomoted over the substrate (Movie 2). Moreover, the fraction of cells forming broad lamellipodial protrusions apparently increased in the caldesmon-transduced cells as compared to control cells (see Figs. 4, 5, and 7).
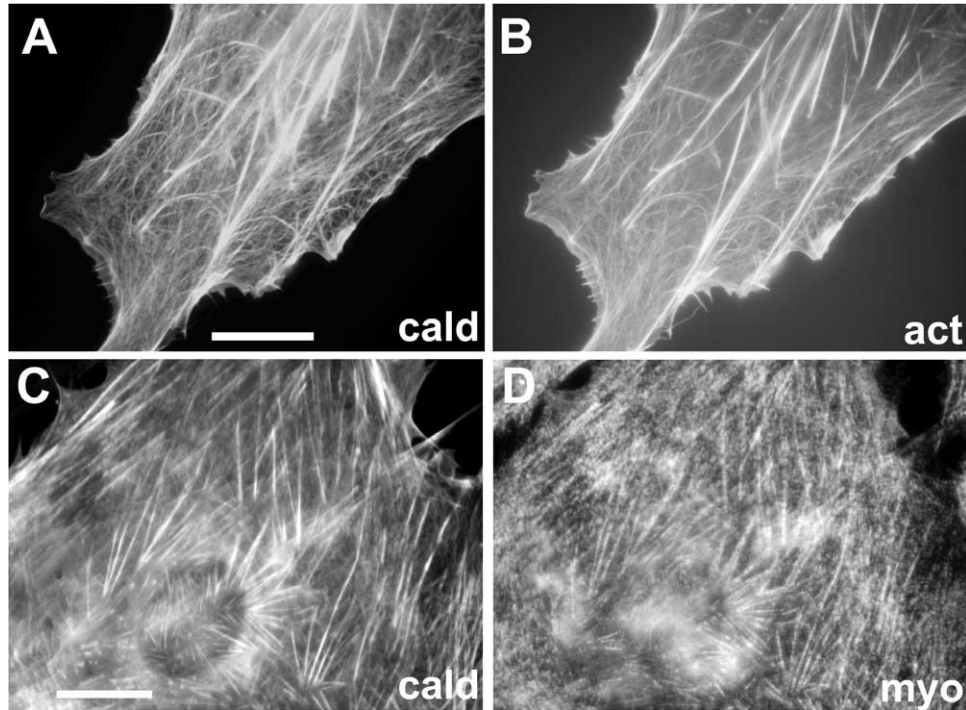
Fig. 2. Localization of GFP-caldesmon to actin- and myosin II-containing structures in cells with moderately perturbed actin cytoskeleton. Two examples of HTM cells infected with adenovirus encoding GFP-caldesmon (AdCaldGFP) are shown. Distributions of GFP-caldesmon (cald) in cells are shown in A and C; distributions of actin (act) corresponding to A and myosin light chain (myo) corresponding to C are shown in B and D, respectively. While some cells contain long stress fibers (A, B), in the majority of cases the fibers are short (C, D), but still contain myosin II in the form of striations (D). Thin curved fibers are often seen between the straight stress fibers (A, B). Caldesmon is enriched in both stress fibers and curved fibers. Scale bars: 10 μm.

Another type of novel actin-containing structure, induced by high caldesmon over-expression were dynamic circular or semi-circular structures (Fig. 4C and D; Movie 1) identified recently in other cell types and known as 'travelling waves', 'clouds', or 'explosions' (Krueger et al., 2003; Bretschneider et al., 2004; Gerisch et al., 2004). These bright circular clusters of small spots positive for both actin and caldesmon (Fig. 4C and D) were transient and rapidly disassembled in the course of centrifugal expansion. The velocity of the wave propagation was very high (in the range of 10 μm per min). We never
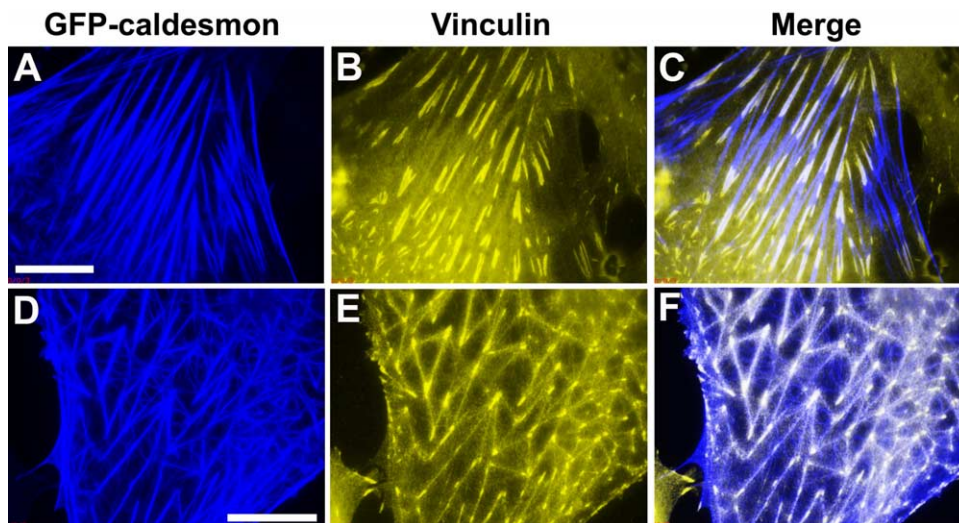

Fig. 3. Organization of the stress fibers and focal adhesions in HTM cells mildly affected by GFP-caldesmon expression. Two cells expressing GFP-caldesmon and stained with vinculin antibody are shown. GFP-caldesmon is shown in blue in A and D; distributions of vinculin in the same cells are shown in yellow (B and E), and merged images are shown in C and F, respectively. Regions of overlap between blue and yellow are seen as white in the merged images. In cells, which preserve apparently intact stress-fibers (A), vinculin-containing FAs are also well preserved (B). Superimposition of GFP-caldesmon and vinculin images (C) reveals that GFP-caldesmon often partially or entirely co-localize with vinculin at FAs. In many GFP-caldesmon expressing cells, stress fibers are short and form triangular networks (D). Vinculin is concentrated in the vertices and shows dim fluorescence along the stress fibers (E). GFP-caldesmon localizes prominently to both stress fibers and vertices (D, F). Thin curved fibers enriched in caldesmon do not contain vinculin (F). Scale bars: 10 μm.
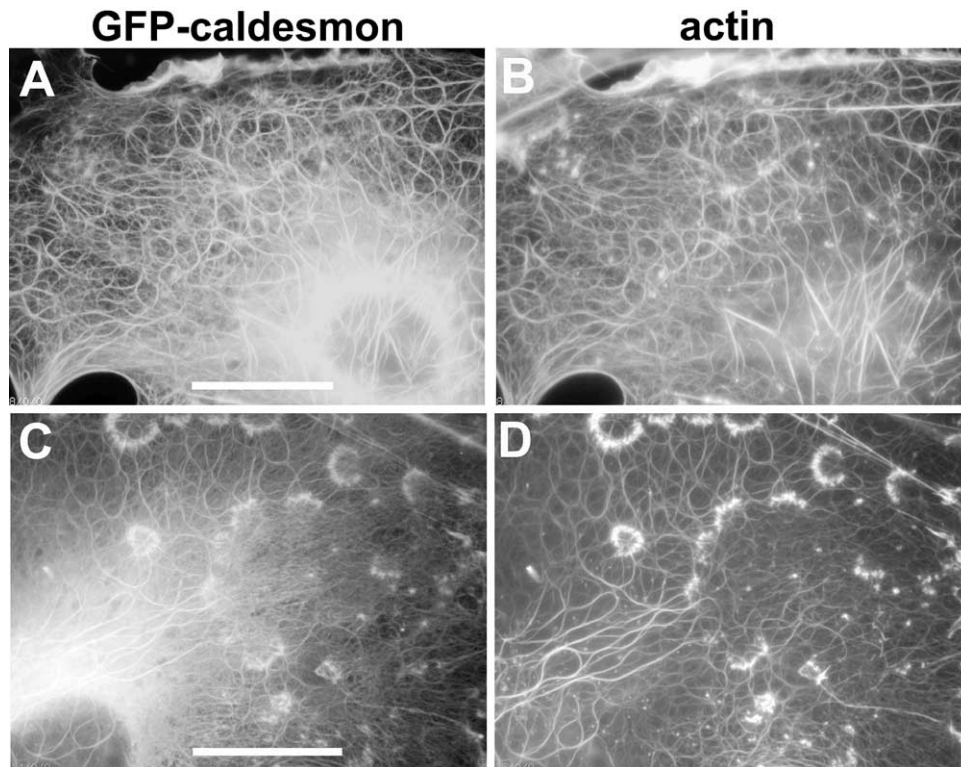
GFP-caldesmon   actin

Fig. 4. Reorganization of the actin cytoskeleton by caldesmon: strongly affected cells. Two HTM cells expressing high levels of GFP-caldesmon are shown. Distributions of GFP-caldesmon are shown in (A) and (C); distributions of actin (visualized by phalloidin) in the same cells—in (B) and (D), respectively. Note that the stress fibers completely disappeared and are substituted by a network of curved actin fibers (B, D). In some cells, numerous actin-rich circular or semi-circular actin waves are clearly seen (D). GFP-caldesmon colocalizes with F-actin in both curved fibers (A, C) and waves (C), as well as in lamellipodia and ruffles at the cell leading edge, seen at the upper part of the photographs (A and B). Scale bars: 10 µm. See also Movies 1 and 2 in the online version of the paper.

observed such structures in control HTM cells, or in caldesmon over-expressing cells, which still retained strong arrays of stress fibers. Formation of such waves seemed to be accompanied by decreased actin fluorescence inside the 'explosion zone'.

3.4. Regulation of caldesmon-induced curvilinear cables by calcium

The curved actin loops still contained myosin II. Staining for myosin light chain did not reveal an apparent decrease in the amount of myosin bound to curved actin fibers as compared to the straight ones (Fig. 5); on the contrary, some 'curvilinear' fibers were apparently more prominent upon myosin than actin staining (Fig. 5C and F). Thus, these completely 'relaxed' structures (as can be inferred from their loose morphology), may still preserve the ability to contract if the inhibitory effect of caldesmon is suppressed.

Since caldesmon activity is negatively regulated by Ca^{++}-calmodulin (Marston et al., 1998; Dabrowska et al., 2004), the effect of increasing intracellular Ca^{++} on the curved actin bundles was examined. Addition of 2 µM thapsigargin, which transiently increases intracellular Ca^{++} concentration (Treiman et al., 1998), resulted in gradual straightening of curved fibers (Fig. 6; Movie 3), presumably by stretching. At the same time the density of caldesmon associated with the fibers was apparently the same in curved

(relaxed) fibers and the stretched, straight ones. Presumably, Ca^{++}-calmodulin suppressed the caldesmon-mediated inhibitory effect on actomyosin bundle contractility, but did not interfere with the association of caldesmon with actin.

3.5. Differential effects of caldesmon over-expression on cell–matrix adhesion structures

In cells with disrupted stress fibers, typical vinculin- and phosphotyrosine-containing FAs were also disrupted (Fig. 7A and B and accompanying paper by Gabelt et al., this volume). Phosphotyrosine-positive focal complexes were still preserved in the lamellipodia (Fig. 7B). In the regions where curved actin fibers were localized, no staining of classical FAs was observed. However, in cells where the stress fibers were still preserved, FAs associated with the ends of these stress fibers were also detected (Fig. 7A and B). In cell regions with curved actin bundles, tensin-positive spot-like structures were often seen, but typical tensin-rich fibrillar adhesions were absent (Fig. 7C and D). Thus, in addition to the conversion of stress fibers into curved fibers, caldesmon over-expression led to disassembly of classical FAs and to dispersion of fibrillar adhesions into scattered, tensin-containing patches. At the same time, focal complexes at the lamellipodia regions were not suppressed, and even accumulated in the caldesmon over-expressing cells.
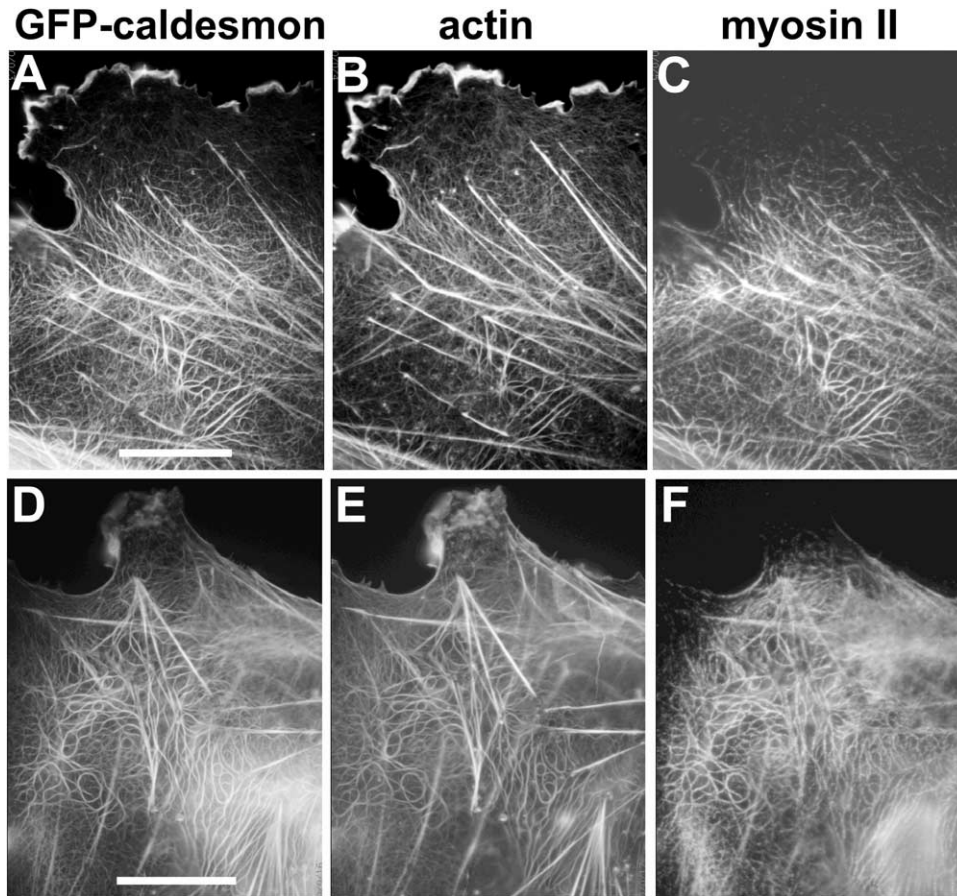
Fig. 5. Actin and myosin II in the caldesmon over-expressing cells. Two GFP-caldesmon-transfected cells are shown (A–C) and (D–F). Distribution of GFP caldesmon is shown in (A) and (D), distribution of actin in (B) and (E), distribution of myosin II light chain in (C) and (F). Both cells demonstrate augmented ruffling at the leading edge and form numerous curved actin fibers. Some residual stress fibers are also seen. Note that GFP-caldesmon is colocalized with actin in all types of structures, while myosin is enriched in stress fibers and curved actin fibers, but is not seen in lamellipodia and ruffles. Scale bars: 10 μm.
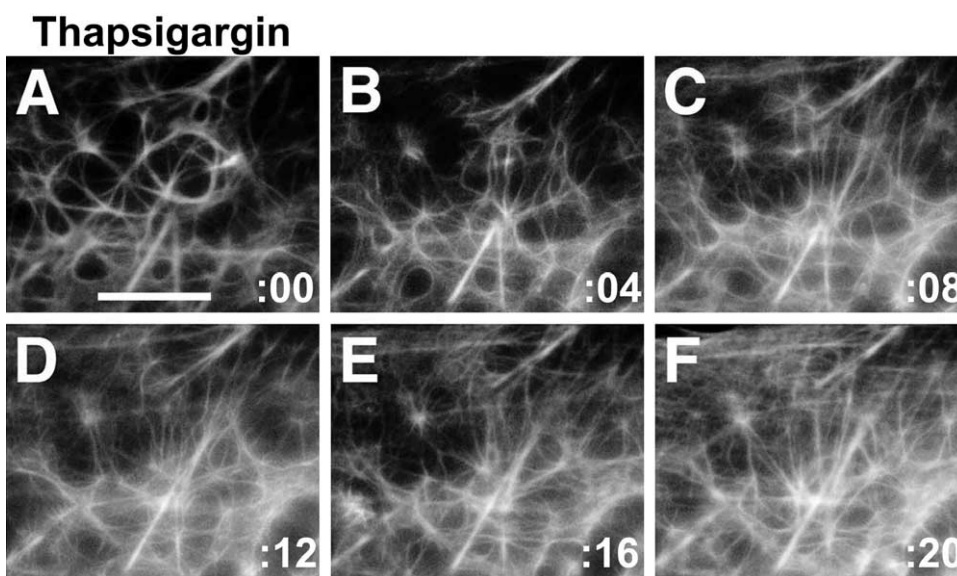
Fig. 6. Recovery of normal actin cytoskeleton structure in caldesmon over-expressing cells upon increase of intracellular calcium concentration. The same part of a GFP-caldesmon-transfected cell is shown immediately after (A), and 4 (B), 8 (C), 12 (D), 16 (E) and 20 (F) min after addition of 2 μM thapsigargin. Note gradual conversion of curved fibers (A) into straight stress-fiber-like actin bundles (F). Scale bar: 5 μm. Fluorescence time-lapse microscopy. See also Movie 3 in the online version of the paper.
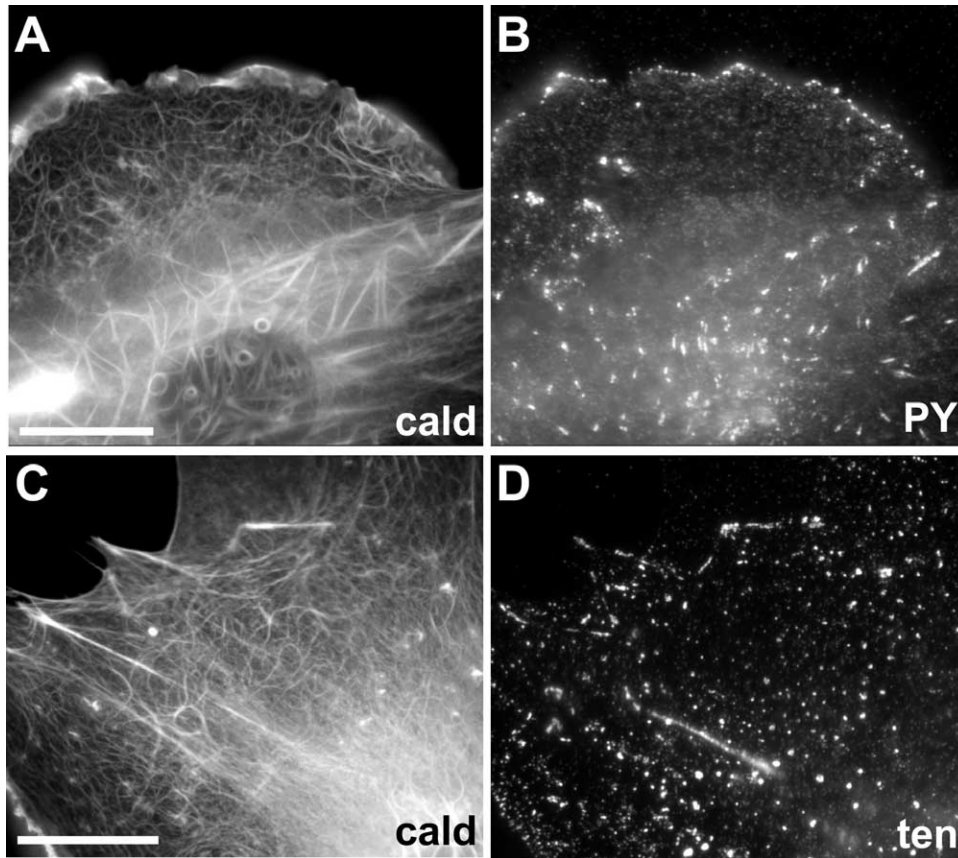
Fig. 7. Effect of caldesmon on different types of cell–matrix adhesions. Two cells expressing GFP-caldesmon (A and C) are stained with antibody to phosphotyrosine (B) and with antibody to tensin (D), respectively. GFP-caldesmon (cald) is localized to curved fibers, residual straight stress fibers, and the dense network in the lamellipodia at the leading edge (A, C). Mature, streak-like focal adhesions are not formed in the cell region with curved fibers, but still can be seen at the ends of the residual stress fibers (A, B). Dot-like focal complexes are accumulated at the cell leading edge (B). Tensin-positive fibrillar adhesions essentially disappeared; instead, numerous tensin spots are seen scattered over the entire cell surface (D). Scale bars: 10 μm.

3.6. Caldesmon-induced destabilization of cell–cell adherens junctions

HTM cells in dense culture form cell–cell junctions (Cai et al., 2000; Liu et al., 2001), but since our experiments were performed in sparse cultures, we were not able to assess the effect of caldesmon over-expression on the intercellular junctions of these cells. To investigate the effect of caldesmon over-expression on adherens junctions, we used epithelial MDCK cells. We have shown that caldesmon over-expression in these cells inhibits cadherin and β-catenin recruitment to cell–cell junctions (Fig. 8A–F and data not shown). Using computer-assisted fluorescence microscopy we examined the dependence of the β-catenin content in the junctions (Fig. 8D–F) on the level of caldesmon expression (Fig. 8A–C). We observed apparent dose dependence in the caldesmon effect: the more caldesmon expressed in the cell, the lower was the amount of β-catenin at the adherens junctions. Quantitation of the intensity of β-catenin labeling in GFP-caldesmon expressing cells demonstrated that β-catenin localization to the junctions in caldesmon transfected cells was decreased up to four fold as compared to the non-transfected cells in the same field (Fig. 8 G). Over-expression, even at relatively high levels, of the non-active, truncated caldesmon, which lacks actin and myosin-binding domains

(Helfman et al., 1999), did not reduce β-catenin labeling in the adherens junctions. High levels of caldesmon expression were correlated with physical disruption of the junctional structure (Fig. 8C and F). At the same time the truncated caldesmon did not induce any changes in adherens junction integrity (data not shown). Thus, modulation of the actin cytoskeleton by caldesmon affected not only formation of cell–extracellular matrix adhesions, but may also play a role in the regulation of cadherin-mediated cell–cell junctions.

4. Discussion

In our previous study (Helfman et al., 1999), we showed that caldesmon over-expression in fibroblasts blocked myosin II-driven contractility and consequently lead to the disappearance of focal adhesions. In the current study, we used adenoviral delivery of GFP-caldesmon to HTM cells, and not only confirmed these results (see accompanying paper by Gabelt et al., this volume), but significantly extended them, revealing entirely new features of the caldesmon effect. Cultured HTM cells are an excellent model for studies of the actin cytoskeleton and cell–matrix adhesions, since these cells are highly spread on the solid substrate and form well-developed
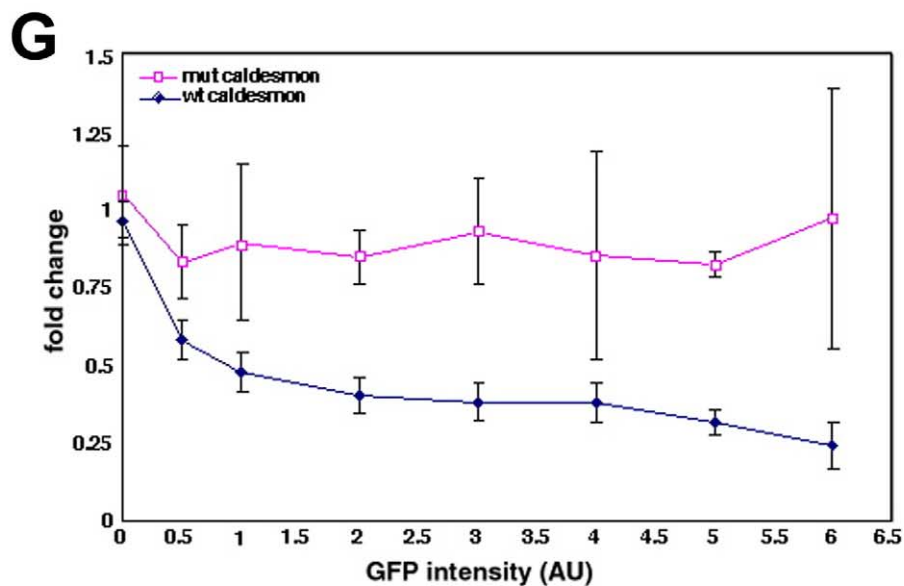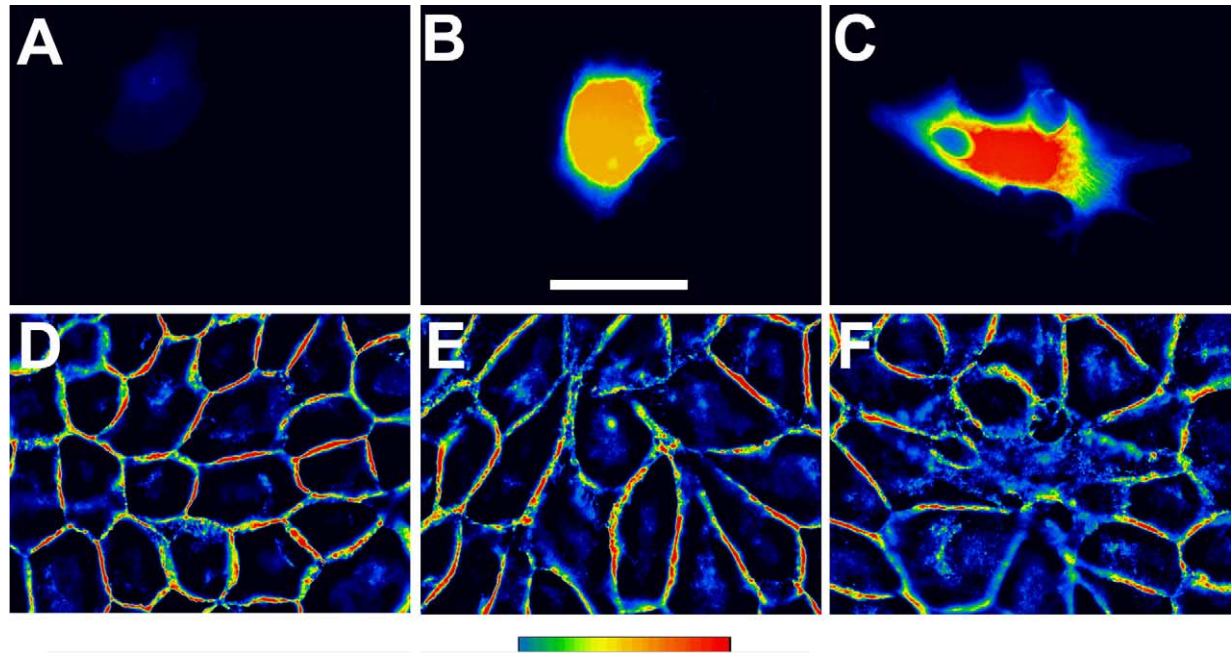
Fig. 8. Effect of caldesmon expression on the cell–cell adherens junctions in MDCK cells. MDCK epithelial cells were transfected with GFP-caldesmon (A–C) and the marker of cell–cell junctions, β-catenin, was visualized by antibody staining (D–F). The relative fluorescence intensities of GFP and β-catenin labeling are presented in a spectrum scale with the highest intensity corresponding to the red color (A–F). Note the decrease in β-catenin contents at the cell–cell adhesion sites in cells expressing high levels of caldesmon (E and F). Scale bar: 20 μm. Integrated intensities of cell contact labeling by β-catenin in GFP-expressing cells were measured as described in Section 2, and normalized to the mean integrated intensity of such labeling in non-transfected cell in the same field (G). GFP intensities in the transfected cells were normalized between the experiments and expressed in arbitrary units (AU). Standard deviations for the results of three independent experiments for full-length caldesmon (more than 100 cells) and two independent experiments for truncated (non-active) caldesmon (about 50 cells) are shown. Note nearly a four-fold decrease in β-catenin labeling in adherens junctions at high levels of full-length GFP-caldesmon expression.

arrays of stress-fibers and associated focal adhesions. We demonstrated that these cells, similarly to trabecular meshwork cells in vivo, express endogenous caldesmon. Therefore the mechanisms of caldesmon-mediated regulation of the cytoskeleton are most probably preserved in these cells. Moreover, the experimental model based on HTM cells allowed us to analyze effects of caldesmon in greater detail than was possible using fibroblasts.

We were able to distinguish two levels of caldesmon action, corresponding to mild and severe reorganization of the actin cytoskeleton. At the mild stage, stress fibers still persisted but became much shorter and formed a triangular network resembling 'geodome'-like structures observed in spreading fibroblast-like cells (Lazarides, 1976), as well as in steroid-treated HTM cells (Clark et al., 2005). Already at this stage, in addition to straight stress fibers, thin, curved fibers, connecting

neighboring stress fibers, were seen. The severe effect, which usually corresponded to a higher level of exogenous caldesmon expression (up to 50-fold according to our rough estimation), was characterized by complete destruction of stress fiber-like structures; curvilinear actin- and caldesmon-containing fibers became prominent. This pattern of actin organization is unique and to our knowledge has not been observed previously.

Formation of both types of actin structures can be attributed to gradual inhibition of myosin II-driven contractility by caldesmon. A triangular actin network was formed when tension was still developing, albeit to a lesser degree than in control cells. Curvilinear actin loops corresponded to the situation of complete loss of tension in the actin network. This interpretation is consistent with our experiments, in which transient recovery of contractility in caldesmon-transfected cells was obtained by thapsigargin-induced Ca^{++} release. In these experiments we observed rapid transitions of curved fibers into straight ones. On the other hand, we never observed formation of such a network of curvilinear fibers in HTM cells treated with chemical inhibitors of myosin II activity (such as H-7 and Y-27632; (Liu et al., 2001)) and our unpublished results). These inhibitors induced complete dissolution of actomyosin bundles in the affected cells. This suggests that the formation of curved fibers depends not only on myosin II inhibition, but on interaction of caldesmon with targets other than myosin II (for example actin and/or tropomyosin). As previously mentioned, caldesmon may regulate actin filament bundling, via competition with fascin (Ishikawa et al., 1998) and by direct cross-linking (Lynch et al., 1987).

It is worth noting that non-contractile curved fibers still contained a high amount of myosin II. This observation suggested that the inhibitory action of caldesmon did not reduce association of myosin II with actin filaments. Furthermore, inhibition of caldesmon by Ca^{++} and consequent restoration of contractile activity did not lead to dissociation of caldesmon from the actin fibers. Altogether these results suggest that caldesmon-mediated myosin regulation cannot be explained by a simple 'flip-flop' model (Sobue et al., 1985, 1988) based on competition for the binding sites on the actin filament. Our results, together with the results of other studies (Lehman, 1986; Helfman et al., 1999; Li et al., 2004), suggest that caldesmon can halt or trigger myosin II activity while remaining, together with myosin, associated with the actin filaments. Another intriguing question is related to the apparent dynamic properties of the curved fibers. What is the origin of such dynamicity in conditions of complete inhibition of myosin II activity? Structural organization, interactions with other cytoskeletal elements, and possible biological function of these curvilinear actin loops deserve further investigation.

Another type of structure induced in HTM cells by caldesmon over-expression were actin 'travelling waves'. These structures are similar to those observed in other cell types upon stimulation with some motogenic factors (such as PDGF) (Krueger et al., 2003), during rapid locomotion (Bretschneider et al., 2004), or the recovery from actin-depolymerizing drugs (Gerisch et al., 2004). Actin waves are in some cases associate with 'dorsal' membrane ruffles, while in other cases with podosomes and invadopodia at the 'ventral' cell surface (Buccione et al., 2004). Mechanisms of their formation and propagation are poorly understood, but are thought to be related to the processes of rapid actin polymerization–depolymerization. Our results suggest an involvement of caldesmon in the formation of these peculiar structures. Both caldesmon-mediated myosin II regulation and its effect on Arp2/3 function might play a role in this effect. Moreover, caldesmon dependence on intracellular calcium may link these actin waves with known cytoplasmic calcium waves.

The effects of caldesmon on matrix adhesions, observed in the present study, and in the accompanying paper (Gabelt et al., this volume) were consistent with our previous results (Helfman et al., 1999), and with results of other investigators (Numaguchi et al., 2003; Li et al., 2004). FAs were most sensitive to caldesmon-induced blockage of contractility, while focal complexes at the lamellipodia were still efficiently formed. A novel finding was the apparent disruption of tensin-rich fibrillar adhesions by caldesmon, observed in this study. Of note, chemical inhibitors of myosin II activity (H7 and ML7) did not disrupt fibrillar adhesions in fibroblasts (Zamir et al., 2000).

Finally, we have clearly demonstrated here that cadherin-mediated cell–cell junctions were also sensitive to caldesmon over-expression. This part of our study was performed in MDCK epithelial cells that display well developed adherens junctions. We showed that β-catenin content in the adherens junctions decreased upon increasing caldesmon concentration. Moreover, high levels of caldesmon over-expression led to physical disruption of the adherens junctions. This effect may be related to myosin II inhibition, as well as to inhibition of Arp2/3-mediated actin nucleation by caldesmon, since both myosin II and Arp2/3 are important for the junctional stability (Verma et al., 2004; Shewan et al., 2005). Again, known effects of chemical inhibitors of myosin II activity on adherens junctions (Volberg et al., 1994; Liu et al., 2001) seem to be significantly weaker than the effects of caldesmon.

In summary, the motivation to test the possible application of caldesmon for glaucoma gene therapy was based on the similarity of its effects to those of chemical inhibitors of myosin function, which were shown to increase outflow facility and decrease IOP (see Section 1). The present study indicates that caldesmon effects are unique and in many ways differ from the effects of these inhibitors. Caldesmon effects also differ from the effects of bacterial C3 toxin (a potent Rho inhibitor) and dominant negative RhoA, which recently were also suggested as potentially interesting treatments (Vittitow et al., 2002; Liu et al., 2005). Gene therapy aimed at inhibiting the Rho-mediated signalling, via over-expression of C3 toxin, disrupts the HTM cell cytoskeleton and increases outflow facility in primate anterior segment organ culture (Liu et al., 2005). Similarly, over-expression of a dominant negative RhoA increases outflow facility in human organ-cultured anterior segments (Vittitow et al., 2002). The common denominator of all these treatments is significant disruption of the stress fibers and focal adhesions. Whether specific

features of caldesmon over-expression (formation of curved actin fibers and actin waves, stronger effects on fibrillar adhesions and on cell–cell junctions) will be beneficial or detrimental for gene therapy is not clear yet and definitely deserves in-depth investigation. The striking effects of caldesmon on the actin organization in HTM cells reveal basic aspects of cytoskeletal regulation in these cells.

Acknowledgements

Appendix. Supplementary Material

Supplementary data associated with this article can be found, in the online version, at doi:10.1016/j.exer.2006.01.006

In all movies, images were taken at 1 min intervals and played back at 10 frames per sec.

References

Bershadsky, A.D., Balaban, N.Q., Geiger, B., 2003. Adhesion-dependent cell mechanosensitivity. Ann. Rev. Cell Dev. Biol. 19, 677–695.

Bretschneider, T., Diez, S., Anderson, K., Heuser, J., Clarke, M., Muller-Taubenberger, A., Kohler, J., Gerisch, G., 2004. Dynamic actin patterns and Arp2/3 assembly at the substrate-attached surface of motile cells. Curr. Biol. 14, 1–10.

Buccione, R., Orth, J.D., McNiven, M.A., 2004. Foot and mouth: podosomes, invadopodia and circular dorsal ruffles. Nat. Rev. Mol. Cell Biol. 5, 647–657.

Burridge, K., Wennerberg, K., 2004. Rho and Rac take center stage. Cell 116, 167–179.

Cai, S., Liu, X., Glasser, A., Volberg, T., Filla, M., Geiger, B., Kaufman, P.L., 2000. Effect of latrunculin-A on morphology and actin-associated adhesions of cultured human trabecular meshwork cells. Mol. Vis. 6, 132–143.

Chalovich, J.M., Sen, A., Resetar, A., Leinweber, B., Fredricksen, R.S., Lu, F., Chen, Y.D., 1998. Caldesmon: binding to actin and myosin and effects on elementary steps in the ATPase cycle. Acta Physiol. Scand. 164, 427–435.

Chrzanowska-Wodnicka, M., Burridge, K., 1996. Rho-stimulated contractility drives the formation of stress fibers and focal adhesions. J. Cell Biol. 133, 1403–1415.

Clark, A.F., Brotchie, D., Read, A.T., Hellberg, P., English-Wright, S., Pang, I.-H., Ethier, C.R., Grierson, I., 2005. Dexamethason alters F-actin architecture and promotes cross-linked actin network formation in human trabecular meshwork tissue. Cell Motil. Cytoskel. 60, 83–95.

Dabrowska, R., Hinssen, H., Galazkiewicz, B., Nowak, E., 1996. Modulation of gelsolin-induced actin-filament severing by caldesmon and tropomyosin and the effect of these proteins on the actin activation of myosin Mg(2+)-ATPase activity. Biochemistry 315, 753–759.

Dabrowska, R., Kulikova, N., Gagola, M., 2004. Nonmuscle caldesmon: its distribution and involvement in various cellular processes. Protoplasma 224, 1–13.

Epstein, D.L., Rowlette, L.-L., Roberts, B.C., 1999. Acto-myosin drug effects and aqueous outflow function. Invest. Ophthalmol. Vis. Sci. 40, 74–81.

Filla, M.S., Liu, X., Nguyen, T.D., Polansky, J.R., Brandt, C.R., Kaufman, P.L., Peters, D.M., 2002. In vitro localization of TIGR/MYOC in trabecular meshwork extracellular matrix and binding to fibronectin. Invest. Ophthalmol. Vis. Sci. 43, 151–161.

Fukata, Y., Amano, M., Kaibuchi, K., 2001. Rho–Rho-kinase pathway in smooth muscle contraction and cytoskeletal reorganization of non-muscle cells. Trends Pharmacol. Sci. 22, 32–39.

Gabelt, B.T., Hu, Y., Vittitow, J.L., Rasmussen, C.R., Grosheva, I., Bershadsky, A.D., Geiger, B., Borrás, T., Kaufman, P.L. Caldesmon transgene expression disrupts focal adhesions in HTM cells and increases outflow facility in organ-cultured human and monkey anterior segments. Exp. Eye Res. 82, this volume.

Geiger, B., Bershadsky, A., Pankov, R., Yamada, K.M., 2001. Transmembrane crosstalk between the extracellular matrix–cytoskeleton crosstalk. Nat. Rev. Mol. Cell Biol. 2, 793–805.

Gerisch, G., Bretschneider, T., Muller-Taubenberger, A., Simmeth, E., Ecke, M., Diez, S., Anderson, K., 2004. Mobile actin clusters and travelling waves in cells recovering from actin depolymerization. Biophys. J. 87, 3493–3503.

Hayashi, K., Yano, H., Hashida, T., Takeuchi, R., Takeda, O., Asada, K., Takahashi, E., Kato, I., Sobue, K., 1992. Genomic structure of the human caldesmon gene. Proc. Natl Acad. Sci. USA 89, 12122–12126.

Helfman, D.M., Lemy, E.T., Berthier, C., Shtutman, M., Riveline, D., Grosheva, I., Lachish-Zalait, A., Elbaum, M., Bershadsky, A.D., 1999. Caldesmon inhibits nonmuscle cell contractility and interferes with the formation of focal adhesions. Mol. Biol. Cell 10, 3097–3112.

Honjo, M., Tankhara, H., Inatani, M., Kido, N., Sawamura, T., Yue, B.Y.J.T., Narumiya, S., Honda, Y., 2001. Effects of rho-associated protein kinase inhibitor Y-27632 on intraocular pressure and outflow facility. Invest. Ophthalmol. Vis. Sci. 42, 137–144.

Huber, P.A., 1997. Caldesmon. Int. J. Biochem. Cell Biol. 29, 1047–1051.

Ishikawa, R., Yamashiro, S., Kohama, K., Matsumura, F., 1998. Regulation of actin binding and actin bundling activities of fascin by caldesmon coupled with tropomyosin. J. Biol. Chem. 273, 26991–26997.

Krueger, E.W., Orth, J.D., Cao, H., McNiven, M.A., 2003. A dynamin–cortactin-Arp2/3 complex mediates actin reorganization in growth factor-stimulated cells. Mol. Biol. Cell 14, 1085–1096.

Lazarides, E., 1976. Actin, alpha-actinin, and tropomyosin interaction in the structural organization of actin filaments in nonmuscle cells. J. Cell Biol. 68, 202–219.

Lehman, W., 1986. Caldesmon association with smooth muscle thin filaments isolated in the presence and absence of calcium. Biochim. Biophys. Acta 885, 88–90.

Li, Y., Wessels, D., Wang, T., Lin, J.L., Soll, D.R., Lin, J.J., 2003. Regulation of caldesmon activity by Cdc2 kinase plays an important role in maintaining membrane cortex integrity during cell division. Cell Mol. Life Sci. 60, 198–211.

Li, Y., Lin, J.L., Reiter, R.S., Daniels, K., Soll, D.R., Lin, J.J., 2004. Caldesmon mutant defective in Ca(2+)-calmodulin binding interferes with assembly of stress fibers and affects cell morphology, growth and motility. J. Cell Sci. 117, 3593–3604.

Liu, X., Cai, S., Glasser, A., Volberg, T., Polansky, J.R., Fauss, D.J., Geiger, B., Kaufman, P.L., 2001. Effect of H-7 on cultured human trabecular meshwork cells. Mol. Vis. 7, 145–153.

Liu, X., Hu, Y., Filla, M.S., Gabelt, B.T., Peters, D.M., Brandt, C.R., Kaufman, P.L., 2005. The effects of C3 transgene expression on actin and cellular adhesions in cultured human trabecular meshwork cells and on outflow facility in organ cultured monkey eyes. Mol. Vis. 11, 1112–1121.

Lynch, W.P., Riseman, V.M., Bretscher, A., 1987. Smooth muscle caldesmon is an extended flexible monomeric protein in solution that can readily undergo reversible intra- and intermolecular sulfhydryl cross-linking. A mechanism for caldesmon's F-actin bundling activity. J. Biol. Chem. 262, 7429–7437.

Manes, T., Zheng, D.Q., Tognin, S., Woodard, A.S., Marchisio, P.C., Languino, L.R., 2003. Alpha(v)beta3 integrin expression up-regulates cdc2, which modulates cell migration. J. Cell Biol. 161, 817–826.

Marston, S., Burton, D., Copeland, O., Fraser, I., Gao, Y., Hodgkinson, J., Huber, P., Levine, B., El-Mezgueidi, M., Notarianni, G., 1998. Structural interactions between actin, tropomyosin, caldesmon and calcium binding protein and the regulation of smooth muscle thin filaments. Acta Physiol. Scand. 164, 401–414.

Murnane, J.P., Fuller, L.F., Painter, R.B., 1985. Establishment and characterization of a permanent pSV ori-transformed ataxia–telangiectasia cell line. Exp. Cell Res. 158, 119–126.

Numaguchi, Y., Huang, S., Polte, T.R., Eichler, G.S., Wang, N., Ingber, D.E., 2003. Caldesmon-dependent switching between capillary endothelial cell growth and apoptosis through modulation of cell shape and contractility. Angiogenesis 6, 55–64.

Okagaki, T., Higashi-Fujime, S., Ishikawa, R., Takano-Ohmuro, H., Kohama, K., 1991. In vitro movement of actin filaments on gizzard smooth muscle myosin: requirement of phosphorylation of myosin light chain and effects of tropomyosin and caldesmon. J. Biochem. 109, 858–866.

Payne, A.M., Yue, P., Pritchard, K., Marston, S.B., 1995. Caldesmon mRNA splicing and isoform expression in mammalian smooth-muscle and non-muscle tissues. Biochem. J. 305, 445–450.

Peterson, J.A., Tian, B.T., Geiger, B., Kaufman, P.L., 1999. Latrunculin (LAT)—A causes mydriasis and cycloplegia in the cynomolgus monkey. Invest. Ophthalmol. Vis. Sci. 40, 631–638.

Peterson, J.A., Tian, B., Geiger, B., Kaufman, P.L., 2000. Effect of latrunculin-B on outflow facility in monkeys. Exp. Eye Res. 70, 307–313.

Rao, P.V., Deng, P.-F., Kumar, J., Epstein, D.L., 2001. Modulation of aqueous humor outflow facility by the Rho kinase-specific inhibitor Y-27632. Invest. Ophthalmol. Vis. Sci. 42, 1029–1037.

Rao, P.V., Deng, P., Sasaki, Y., Epstein, D.L., 2005. Regulation of myosin light chain phosphorylation in the trabecular meshwork: role in aqueous humour outflow facility. Exp. Eye Res. 80, 197–206.

Riveline, D., Zamir, E., Balaban, N.Q., Schwarz, U.S., Ishizaki, T., Marumiya, S., Kam, Z., Geiger, B., Bershadsky, A.D., 2001. Focal contacts as mechanosensors: externally applied local mechanical force induces growth of focal contacts by an mDia1-dependent and ROCK-independent mechanism. J. Cell Biol. 153, 1175–1186.

Shewan, A.M., Maddugoda, M., Kraemar, A., Stehbens, S.J., Verma, S., Kovacs, E.M., Yap, A.S., 2005. Myosin 2 is a key Rho kinase target necessary for the local concentration of E-cadherin at cell–cell contacts. Mol. Biol. Cell 16, 4531–4542.

Shirinsky, V.P., Biryukov, K.G., Hettasch, J.M., Sellers, J.R., 1992. Inhibition of the relative movement of actin and myosin by caldesmon and calponin. J. Biol. Chem. 267, 15886–15892.

Small, J.V., Stradal, T., Vignal, E., Rottner, K., 2002. The lamellipodium: where motility begins. Trends Cell Biol. 12, 112–120.

Sobue, K., Takahashi, K., Wakabayashi, I., 1985. Caldesmon150 regulates the tropomyosin-enhances actin–myosin interaction in gizzard smooth muscle. Biochem. Biophys. Res. Comm. 132, 645–651.

Sobue, K., Kanda, K., Tanaka, T., Ueki, N., 1988. Caldesmon: a common actin-linked regulatory protein in the smooth muscle and nonmuscle contractile system. J. Cell Biochem. 37, 317–325.

Svitkina, T.M., Neyfakh, A.A.J., Bershadsky, A.D., 1986. Actin cytoskeleton of spread fibroblasts appears to assemble at the cell edges. J. Cell Sci. 82, 235–248.

Tian, B., Kaufman, P.L., 2005. Effects of the rho kinase inhibitor Y-27632 and the phosphatase inhibitor calyculin-A on outflow facility in monkeys. Exp. Eye Res. 80, 215–225.

Tian, B., Brumback, L.C., Kaufman, P.L., 2000. ML-7, chelerythrine and phorbol ester increase outflow facility in the monkey eye. Exp. Eye Res. 71, 551–566.

Tian, B., Wang, R.-F., Podos, S.M., Kaufman, P.L., 2004. Effects of topical H-7 on outflow facility, intraocular pressure and corneal thickness in monkeys. Arch. Ophthalmol. 122, 1171–1177.

Treiman, M., Caspersen, C., Christensen, S.B., 1998. A tool coming of age: thapsigargin as an inhibitor of sarco-endoplasmic reticulum $Ca(2+)$-ATPases. Trends Pharmacol. Sci. 19, 131–135.

Verkhovsky, A.B., Svitkina, T.M., Borisy, G.G., 1995. Myosin II filament assemblies in the active lamella of fibroblasts: their morphogenesis and role in the formation of actin filament bundles. J. Cell Biol. 131, 989–1002.

Verma, S., Shewan, A.M., Scott, J.A., Helwani, F.M., den Elzen, N.R., Miki, H., Takenawa, T., Yap, A.S., 2004. Arp2/3 activity is necessary for efficient formation of E-cadherin adhesive contacts. J. Biol. Chem. 279, 34062–34070.

Vittitow, J.L., Garg, R., Rowlette, L.L., Epstein, D.L., O'Brien, E.T., Borrás, T., 2002. Gene transfer of dominant-negative RhoA increases outflow facility in perfused human anterior segment cultures. Mol. Vis. 8, 32–44.

Volberg, T., Geiger, B., Citi, S., Bershadsky, A.D., 1994. Effect of protein kinase inhibitor H-7 on the contractility, integrity and membrane anchorage of the microfilament system. Cell Motil. Cytoskel. 29, 321–338.

Yamakita, Y., Oosawa, F., Yamashiro, S., Matsumura, F., 2003. Caldesmon inhibits Arp2/3-mediated actin nucleation. J. Biol. Chem. 278, 17937–17944.

Yamashiro, S., Chern, H., Yamakita, Y., Matsumura, F., 2001. Mutant caldesmon ladking cdc2 phosphrylation sites delays M-phase entry annd inhibits cytokinesis. Mol. Biol. Cell 12, 239–250.

Yoneda, A., Multhaupt, H.A., Couchman, J.R., 2005. The Rho kinases I and II regulate different aspects of myosin II activity. J. Cell Biol. 170, 443–453.

Zamir, E., Katz, B.Z., Aota, S., Yamada, K.M., Geiger, B., Kam, Z., 1999. Molecular diversity of cell–matrix adhesions. J. Cell Sci. 112, 1655–1669.

Zamir, E., Katz, M., Posen, Y., Erez, N., Yamada, K.M., Katz, B.Z., Lin, S., Lin, D.C., Bershadsky, A., Kam, Z., Geiger, B., 2000. Dynamics and segregation of cell–matrix adhesions in cultured fibroblasts. Nat. Cell Biol. 2, 191–196.